

Synthesis of a ^{11}C -Isotopologue of the B-Raf-Selective Inhibitor Encorafenib Using In-Loop $[^{11}\text{C}]\text{CO}_2$ Fixation

Mark H. Dornan,* Daniil Petrenyov, José-Mathieu Simard, Mehdi Boudjemeline, Roxana Mititelu, Jean N. DaSilva, and Anthony P. Belanger



Cite This: *ACS Omega* 2020, 5, 20960–20966

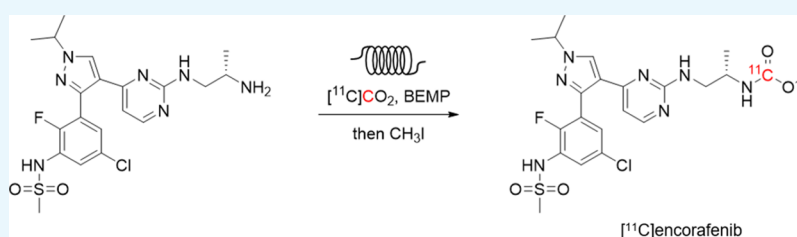


Read Online

ACCESS |

Metrics & More

Article Recommendations



ABSTRACT: The serine/threonine kinase B-Raf is an essential regulator of cellular growth, differentiation, and survival. B-Raf protein expression is elevated throughout melanoma progression, making it an attractive target for noninvasive imaging using positron-emission tomography. Encorafenib is a potent and highly selective inhibitor of B-Raf used in the clinical management of melanoma. In this study, the radiosynthesis of a ^{11}C -isotopologue of encorafenib was developed using an in-loop $[^{11}\text{C}]\text{CO}_2$ fixation reaction. Optimization of reaction conditions reduced the formation of a radiolabeled side product and improved the isolated yields of $[^{11}\text{C}]\text{encorafenib}$ ($14.5 \pm 2.4\%$ radiochemical yield). The process was fully automated using a commercial radiosynthesizer for the production of 6845 ± 888 MBq of $[^{11}\text{C}]\text{encorafenib}$ in high molar activity (177 ± 5 GBq μmol^{-1}), in high radiochemical purity (99%), and in a formulation suitable for animal injection. An *in vitro* cellular binding experiment demonstrated saturable binding of the radiotracer to A375 melanoma cells.

1. INTRODUCTION

Melanoma is an aggressive form of skin cancer, which accounted for approximately 59,782 deaths and 351,880 new patients worldwide in 2015.^{1,2} Although localized melanoma is highly curable, patients diagnosed with metastatic disease face a 25% 5-year survival rate.³ This underscores the need for new strategies for detection, accurate prognosis assessment, and methods to predict response to therapies.

The protein B-Raf (encoded by the gene BRAF) is an oncogenic serine/threonine kinase, which plays a pivotal role in the MAPK/ERK signal transduction pathway, a regulator of cell differentiation, proliferation, and survival.⁴ Interestingly, studies have shown that B-Raf levels are significantly increased throughout the progression of melanoma in both wild-type and BRAF-mutated tumors.^{5–8} Elevated B-Raf was observed in both primary and metastatic lesions and associated with aggressive tumor features and reduced survival. This hints at a potential prognostic value that B-Raf protein expression may provide.

BRAF is altered in about half of melanomas with V600E being the most common mutation (accounting for approximately 75% of BRAF-mutated melanoma).^{9,10} The high incidence rate of BRAF^{V600E} has led to the development of targeted B-Raf therapeutics, and to date, three B-Raf inhibitors

(vemurafenib, dabrafenib, and encorafenib) have received FDA approval for the treatment of BRAF^{V600E} melanoma. Properties that distinguish encorafenib from other agents in its class are that it has a similar half-maximal inhibitory concentration (IC_{50}) for both wild-type and V600E B-Raf in biochemical assays (0.47 and 0.35 nM, respectively), and a significantly longer B-Raf dissociation half-life ($T_{1/2} > 30$ h) compared with vemurafenib (0.5 h) and dabrafenib (2 h).^{11–13} A positron-emitting tomography (PET) imaging agent derived from encorafenib has the potential for quantitative imaging of B-Raf expression in both BRAF^{V600E} and BRAF^{wt} melanoma. The long-dissociation half-life could allow for the development of a tracer with a slow wash-out rate and a high target retention time.

Three B-Raf-targeted PET radiotracers have been previously reported including a ^{11}C -labeled pyrazolopyridine-based inhibitor, $[^{11}\text{C}]\text{vemurafenib}$, and $[^{11}\text{C}]\text{CEP-32496}$ (Figure

Received: May 22, 2020

Accepted: July 28, 2020

Published: August 16, 2020



1).^{14–17} [¹¹C]Vemurafenib was shown to have high *in vitro* binding to Colo829 (BRAF^{V600E}) and MeWo (BRAF^{wt})

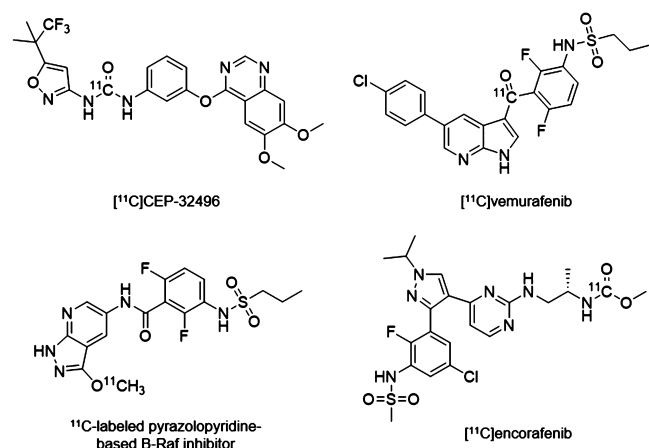


Figure 1. Previously developed B-Raf-targeted PET radiotracers and the proposed structure of [¹¹C]encorafenib.

melanoma cells. Saturable binding was also measured in Colo829 and MeWo xenograft sections by autoradiography. Biodistribution studies of [¹¹C]vemurafenib in mouse xenografts showed modest tumor uptake ($0.87 \pm 0.14\%$ ID/g in Colo829 xenografts, and $0.49 \pm 0.29\%$ ID/g in MeWo xenografts at 60 min postinjection). The *in vitro* evaluation of [¹¹C]CEP-32496 demonstrated high *in vitro* uptake and specificity in A375 (BRAF^{V600E}) melanoma cells and tumor sections, although *in vivo* accumulation of [¹¹C]CEP-32496 in tumor xenografts was low ($1.85 \pm 0.09\%$ ID/g at 60 min postinjection).

To realize PET imaging of B-Raf expression in melanoma, new strategies are needed to improve tumor-to-background signal ratios and increase the total and specific tumor uptake. A radiotracer derived from encorafenib could offer a path to improve PET imaging of B-Raf expression based on its distinct pharmacological properties.^{11,12} In this report, we describe the development and optimization of the radiosynthesis of [¹¹C]encorafenib, constructed using an in-loop [¹¹C]CO₂ fixation reaction. The radiosynthesis, purification, and reformulation were fully automated to enable reproducible and large-scale preparation of [¹¹C]encorafenib in high molar activity. Preliminary *in vitro* evaluation of the radiotracer was completed using A375 melanoma cells.

2. RESULTS AND DISCUSSION

Encorafenib could theoretically be labeled with the PET isotopes carbon-11 ($t_{1/2} = 20.4$ min) or fluorine-18 ($t_{1/2} = 109.8$ min). To label the aryl-fluoride with fluorine-18, a radiochemical precursor with a suitable leaving group at the correct aromatic position would be needed and would require a multistep synthetic approach. To label encorafenib with carbon-11, it was hypothesized that a [¹¹C]CO₂ fixation reaction developed by Wilson and co-workers could be used to easily radiolabel the carbonyl of the methylcarbamate fragment.¹⁸ In this reaction, [¹¹C]CO₂ is trapped and reacted with a CO₂ fixation base and a precursor amine to form a ¹¹C-labeled carbamate ion intermediate. Addition of iodomethane results in alkylation of the carbamate ion to form the methylcarbamate. The required amine precursor **2** to prepare [¹¹C]encorafenib (**[¹¹C]1**) through this reaction could be synthesized in one step from isotopically unmodified encorafenib (**1**) with sodium hydroxide at 85 °C allowed for hydrolysis and decarboxylation of the methyl carbonate to form the corresponding primary amine **2**, which was then purified by high-performance liquid chromatography (HPLC) and isolated as the trifluoroacetic acid (TFA) salt in good yield (81%). Hydrolysis of the native methyl carbamate offered a time- and cost-efficient strategy to prepare the radiochemical precursor for the synthesis of [¹¹C]encorafenib.

The preparation of ¹¹C-labeled radiotracers using in-loop [¹¹C]CO₂ fixation is an established synthesis method.^{18,19} Use of the loop increases the surface area to maximize the gas–liquid contact and the [¹¹C]CO₂ trapping efficiency in small quantities of reagents and simplifies the production process. In 2018, Dahl and co-workers reported an in-loop [¹¹C]CO₂ fixation apparatus designed as a standalone HPLC injector valve that could be integrated with a commercial radio-synthesizer for the automated production of ¹¹C-carbonyl-labeled carbamates and ureas.²⁰ To synthesize [¹¹C]encorafenib (**[¹¹C]1**), a modified version of this procedure was adapted. The Procab and TRACERlab FX2 C chemistry systems were configured in series for the transfer of purified [¹¹C]CO₂ from the molecular sieve column to the loop reactor (**Figure 3**). The loop reactor was charged with a dimethylformamide (DMF) solution of **2** and the CO₂ fixation base 2-*tert*-butylimino-2-diethylamino-1,3-dimethylperhydro-1,3,2-diazaphosphorine (BEMP), enabling formation of the ¹¹C-carbamate ion intermediate (**Figure 2B**). Transfer from the

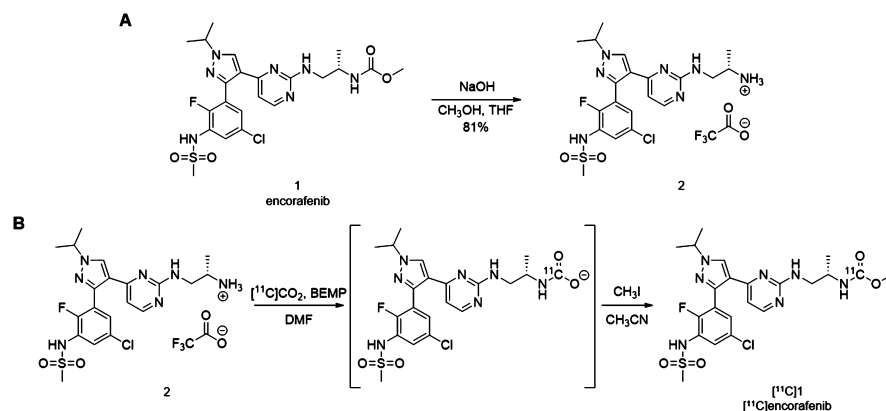


Figure 2. (A) Synthesis of the radiochemical precursor **2**; (B) radiosynthesis of [¹¹C]encorafenib by [¹¹C]CO₂ fixation/alkylation.

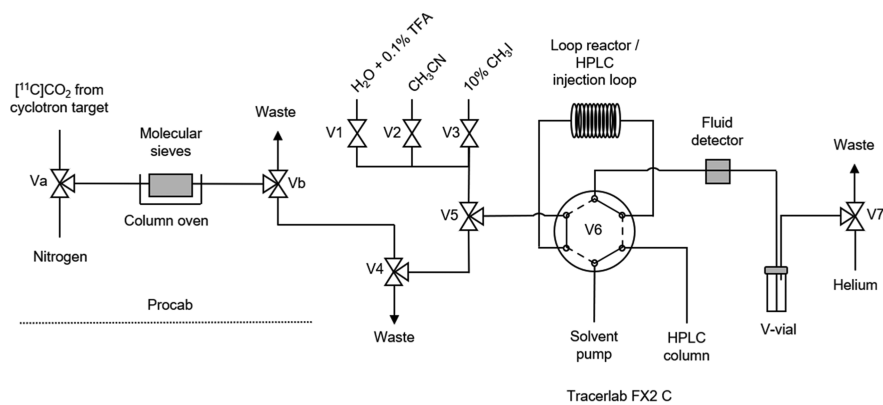


Figure 3. Schematic drawing of the radiosynthesizer configured for $[^{11}\text{C}]$ encorafenib production.

molecular sieve column to the loop reactor took approximately 4 min as measured by monitoring radioactivity detectors proximal to the loop reactor. Iodomethane solution was then passed through the loop for alkylation of the ^{11}C -carbamate ion intermediate. Acetonitrile and water were added sequentially to flush the contents into a V-vial and quench the reaction allowing for adjustment of the solution for HPLC purification. The reaction mixture was back-loaded into the loop and injected onto the semi-preparative HPLC. The fraction containing $[^{11}\text{C}]$ encorafenib was diluted in water, and reformulation was completed using a C18 solid-phase extraction (SPE) cartridge. The SPE trap, wash, and release conditions allowed for the recovery of approximately 73% of the radiotracer from the HPLC mobile phase into a solution of 10% ethanol in 0.9% saline. The described configuration uses the HPLC sample loop of the TRACERlab FX2 C module as both the reactor loop and the HPLC sample injection loop. This offers a simplified process for fully automated production of radiotracers by in-loop $[^{11}\text{C}]\text{CO}_2$ fixation/alkylation reactions requiring minor reconfiguration of the radiosynthesizer (Figure 3).

Reaction optimization of $[^{11}\text{C}]$ encorafenib production using the automated $[^{11}\text{C}]\text{CO}_2$ fixation/alkylation sequence was completed by screening the concentrations of the precursor material **2**, the CO_2 fixation agent BEMP, the total reaction volume preloaded in the loop reactor, and the concentration of the iodomethane solution (Table 1). All test reactions were evaluated by measuring the radiochemical yield (RCY) of

Table 1. Optimization of Reaction Conditions for Production of $[^{11}\text{C}]$ encorafenib

entry	BEMP (μmol)/conc. (mM)	Precursor (μmol)/conc. (mM)	volume (μL)	% CH_3I in CH_3CN	RCY (%) ^a
1	6.9/115	22/1.32	60	10	5.0
2	13.8/230	22/1.32	60	10	6.7
3	20.7/345	22/1.32	60	10	5.3
4	27.6/460	22/1.32	60	10	0
5	13.8/230	11/0.66	60	10	3.0
6	13.8/230	44/2.64	60	10	7.9
7	23/230	44/4.4	100	10	8.7
8	23/230	44/4.4	100	5	11.1
9	23/230	44/4.4	100	2.5	14.5 \pm 2.4 ^b
10	23/230	44/4.4	100	1	10.1

^aRadiochemical yield, isolated ($n = 1$). ^b $n = 3$.

$[^{11}\text{C}]$ encorafenib isolated after purification and reformulation. It was determined that using 23 μmol of BEMP, 44 μmol of the precursor, and increasing the sample volume loaded into the loop reactor to 100 μL (Table 1, entry 7) allowed for a modest improvement of the isolated RCY, reaching 8.7%.

Inspection of the semi-preparative HPLC gamma detector chromatogram (Figure 4) indicated that a major component of

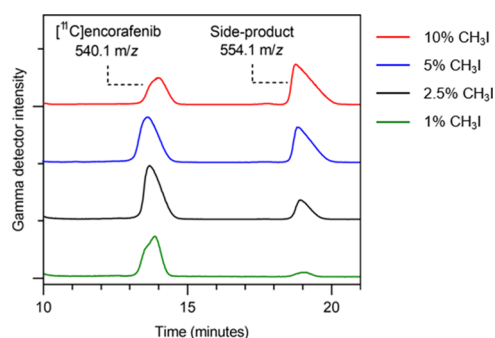


Figure 4. Reducing the concentration of iodomethane to 2.5% leads to improved $[^{11}\text{C}]$ encorafenib yield and limits the formation of the radiolabeled side-product.

the reaction mixture could be attributed to a radiolabeled side-product ($t_R = 18.9$ min), which eluted from the column after the desired product. To identify this compound, fractions containing $[^{11}\text{C}]$ encorafenib and the ^{11}C -labeled side-product were isolated and analyzed by liquid chromatography–mass spectrometry (LC–MS). Nonradioactive encorafenib was detected in the product fraction as the predominant ion ($[M + H]^+ = 540.1$ m/z) as expected while the predominant ion in the side-product fraction was found to be 554.1 m/z . This suggested that the side-product could be formed from a second addition of a methyl group during the alkylation reaction through a reaction between $[^{11}\text{C}]$ encorafenib and excess iodomethane, likely an amino–alkylation reaction. Decreasing the iodomethane concentration in the alkylation reaction to 2.5% resulted in a lower proportion of the radiolabeled side-product formed in the reaction (Figure 4) and improved the yield of $[^{11}\text{C}]$ encorafenib (Table 1, entries 7–10). With 1% iodomethane, formation of the side-product was minimized, although production of $[^{11}\text{C}]$ encorafenib was also reduced.

It was then hypothesized that formation of the side-product by the continued reaction of $[^{11}\text{C}]$ encorafenib with excess iodomethane could be occurring in the V-vial after the loop was flushed with acetonitrile. To investigate this, water (1 mL)

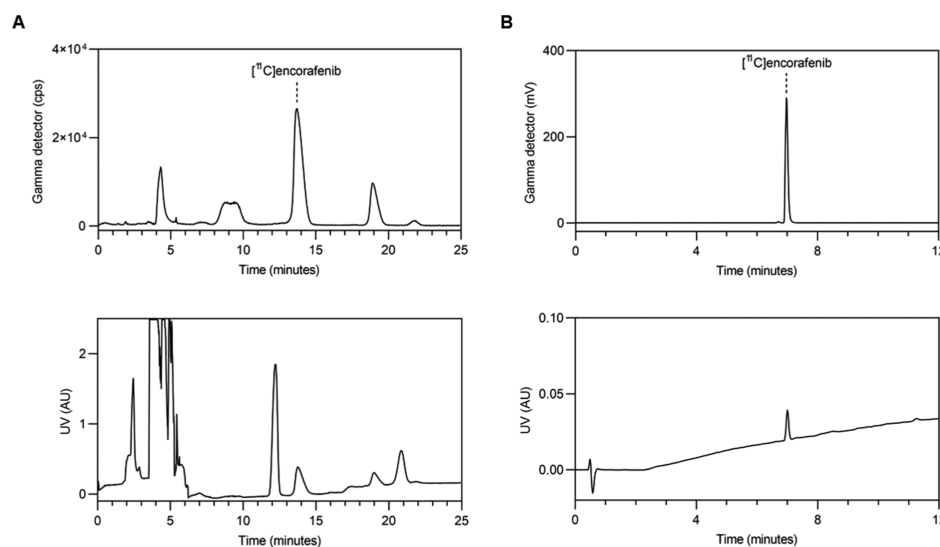


Figure 5. (A) Semi-preparative radio-HPLC chromatogram of $[^{11}\text{C}]$ encorafenib. Top panel: gamma detector ($[^{11}\text{C}]$ encorafenib $t_{\text{R}} = 13.8$ min), bottom panel: UV detector ($\lambda = 254$ nm); (B) analytical radio-HPLC chromatogram of $[^{11}\text{C}]$ encorafenib. Top panel: Gamma detector ($[^{11}\text{C}]$ encorafenib $t_{\text{R}} = 6.9$ min), bottom panel: UV detector ($\lambda = 220$ nm).

was placed in the V-vial to quench the reaction immediately after the loop was flushed. With this method, a comparable RCY of $[^{11}\text{C}]$ encorafenib (15.5%) and proportion of the side-product were observed using the optimized reaction conditions. This indicated that both the radiotracer and the radiolabeled side-product are formed in the loop.

With the optimized reaction conditions, three consecutive production runs were completed to evaluate the capacity of the process to run at a larger scale, the reproducibility of the process, and the radiochemical stability of the final product. Starting from 144 GBq of $[^{11}\text{C}]\text{CO}_2$ at end-of-bombardment, $6,845 \pm 888$ MBq of $[^{11}\text{C}]$ encorafenib was produced at the end-of-synthesis ($14.5 \pm 2.4\%$ isolated RCY, $n = 3$) in 30–35 min. The trapping efficiency of $[^{11}\text{C}]\text{CO}_2$ in the loop was 70%. Typical semi-preparative and analytical HPLC chromatograms are shown in Figure 5. The molar activity was 177 ± 5 GBq μmol^{-1} at the end-of-synthesis ($n = 3$) as determined by analytical HPLC. The pH was consistently measured to be 5.0, and gas chromatography analysis for residual solvents showed that acetonitrile was between 4 and 15 ppm. The radiochemical purity ranged from 98.9 to 99.3%, and no decomposition was detected in analyses of the product 1 h after production at room temperature. Throughout development and validation testing, the method was found to be robust and reliable. This demonstrates that the developed process for $[^{11}\text{C}]$ encorafenib is reproducible and enables the preparation of a stable formulation of $[^{11}\text{C}]$ encorafenib suitable for *in vitro* and *in vivo* studies.

Preliminary evaluation of $[^{11}\text{C}]$ encorafenib was completed using an *in vitro* cellular binding experiment with A375 cells, a human melanoma cell line that expresses V600E-mutated B-Raf and is sensitive to treatment with encorafenib *in vitro* ($\text{EC}_{50} = 4$ nM).^{11,21} Following incubation with $[^{11}\text{C}]$ encorafenib, the cells were washed and transferred for analysis with a gamma counter. The $[^{11}\text{C}]$ encorafenib cellular binding was $0.83 \pm 0.03\%$ ID/mg protein. When the radiotracer was incubated in the presence of an excess amount of non-radioactive encorafenib ($5 \mu\text{M}$), binding was reduced by 49% to $0.41 \pm 0.04\%$ ID/mg protein ($P = 0.0004$). This provides evidence for saturable binding of $[^{11}\text{C}]$ encorafenib to B-Raf in

A375 cells, although a significant amount of nondisplaceable binding remained. These results are comparable with the *in vitro* binding data reported for previously developed B-Raf-targeting PET radiotracers: $[^{11}\text{C}]\text{CEP-32496}$ cell binding was reduced by 50% when incubated with unlabeled CEP-32496 ($10.3 \mu\text{M}$), and $[^{11}\text{C}]\text{vemurafenib}$ cellular binding was reduced from 74.3 ± 1.5 and $61.6 \pm 8.2\%$ in Colo829 and MeWo cells to 17.0 ± 2.3 and $20.6 \pm 0.4\%$ when incubated with vemurafenib ($1 \mu\text{M}$), respectively.^{15,17}

3. CONCLUSIONS

$[^{11}\text{C}]$ Encorafenib was successfully synthesized using in-loop $[^{11}\text{C}]\text{CO}_2$ fixation to label the carbonyl of the methyl carbamate. A simplified procedure was developed to enable $[^{11}\text{C}]\text{CO}_2$ fixation labeling, purification, and reformulation using a commercially available radiosynthesizer. Optimization studies identified reaction conditions to improve the $[^{11}\text{C}]$ encorafenib RCY by reducing the formation of a radiolabeled side-product. Automation of the radiosynthesis process allows for reproducible production of $[^{11}\text{C}]$ encorafenib in high purity, high molar activity, and with sufficient yield to support *in vitro* studies. A preliminary *in vitro* assay demonstrated saturable binding of $[^{11}\text{C}]$ encorafenib to A375 melanoma cells, encouraging further investigations of this radiotracer.

4. METHODS

4.1. Materials. All commercially available materials were used without further purification unless otherwise noted. Encorafenib **1** was purchased from MedChemExpress. ^1H and ^{13}C NMR spectra were acquired with a Bruker AVANCE III HD 600 MHz spectrometer. Spectral data are reported in parts per million using the residual solvent as a reference. High-resolution mass spectrometry was performed by direct injection electrospray ionization (ESI) in positive-ion mode using a Q-Exactive Plus Orbitrap mass spectrometer (HRMS). LC-MS (ESI) was performed using a Waters Acquity Arc UHPLC with an Acquity QDa mass detector in positive-ion mode.

A GE Healthcare Process Cabinet (Procab) was used to purify $[^{11}\text{C}]\text{CO}_2$ from the target gas using a column packed

with molecular sieves (4 Å, 80/100 mesh). Validation of the Procab efficiency demonstrated near-quantitative trap and release of cyclotron produced [^{11}C]CO₂. A GE Healthcare TRACERlab FX2 C radiosynthesizer was used for automated production of [^{11}C]encorafenib. A 1 mL stainless-steel sample loop (1/16" OD, 0.75 mm ID, Vici #SLIKUW) and a 2 mL stainless-steel sample loop (1/16" OD, 0.75 mm ID, Vici #SL2KUW) were connected in series using a union (Vici #ZU1) and installed on the TRACERlab FX2 C HPLC sample injection valve. An injection syringe fill port (Vici #VISF-2) was used to load reagents into the loop reactor through the union. Columns packed with sodium hydroxide-coated silica (Thomas Ascarite II) were connected to the waste ports of the TRACERlab FX2 C radiosynthesizer. Waters Sep-Pak Plus short C18 cartridges (360 mg) were preconditioned by passing through ethanol (10 mL), followed by water (20 mL). A Phenomenex Luna C18(2) column (250 × 10 mm, 10 μm) was used for semi-preparative HPLC purification of the radiochemical precursor. Semi-preparative HPLC purification of [^{11}C]encorafenib was completed with a Phenomenex Luna C18(2) column (250 × 10 mm, 5 μm). A Waters Cortecs C18 column (50 × 4.6 mm, 2.7 μm) was used for analytical HPLC using Waters Acquity Arc UHPLC with a radioactivity detector.

A375 cells (ATCC CRL-1619) were incubated and maintained at 37 °C with 5% CO₂. Dulbecco's modified Eagle medium supplemented with 10% fetal bovine serum and 1% penicillin/streptomycin was used for growth media. Dulbecco's phosphate-buffered saline (DPBS) was used to wash the cells. A PerkinElmer Wizard2 was used to count carbon-11 activity. Protein quantification was completed using a Micro BCA (bicinchoninic acid) Protein Assay kit (Thermo Fischer Scientific).

4.2. Chemistry. 4.2.1. (*S*)-*N*-(3-(4-(2-((2-Aminopropyl)-amino)pyrimidin-4-yl)-1-isopropyl-1*H*-pyrazol-3-yl)-5-chloro-2-fluorophenyl)methanesulfonamide (Compound 2). Encorafenib **1** (20 mg, 0.037 mmol) was dissolved in 10% NaOH_(aq) (1 mL), CH₃OH (1 mL), and tetrahydrofuran (1 mL) in a round-bottom flask equipped with a magnetic stir bar. The solution was heated to 85 °C for 12 h. The crude mixture was concentrated, dissolved in 10% CH₃CN/H₂O + 0.1% TFA, and filtered (0.22 μm). The radiochemical precursor **2** was purified by semi-preparative HPLC (flow rate: 10 mL min⁻¹; 10% CH₃CN/H₂O + 0.1% TFA from 0 to 2 min, 10 to 35% CH₃CN/H₂O + 0.1% TFA from 2 to 12 min, 35% CH₃CN/H₂O + 0.1% TFA from 12 to 15 min). The HPLC fractions containing the desired product were combined, concentrated, resuspended in deionized H₂O, and lyophilized to obtain the final product as a TFA salt of compound **2** (17.7 mg, 0.030 mmol, 81% yield). ¹H NMR (600 MHz, MeOD): δ 8.55 (s, 1H), 8.21 (d, *J* = 5.3 Hz, 1H), 7.60 (dd, *J* = 6.2, 2.4 Hz, 1H), 7.38 (dd, *J* = 5.3, 2.5 Hz, 1H), 6.96 (brs, 1H), 4.66 (sept, *J* = 6.7 Hz, 1H), 3.39–3.31 (m, 2H), 3.28–3.17 (m, 1H), 3.07 (s, 3H), 1.59 (d, *J* = 6.7 Hz, 6H), 1.17 (d, *J* = 4.9 Hz, 3H). ¹³C NMR (151 MHz, MeOD): δ 165.35, 162.77 (q, *J*_{C,F} = 33.5 Hz, TFA), 159.09, 158.81, 152.63 (d, *J*_{C,F} = 250.0 Hz), 151.73, 144.98, 132.59, 130.33 (d, *J*_{C,F} = 2.7 Hz), 128.45 (d, *J*_{C,F} = 15.2 Hz), 128.06, 125.93 (d, *J*_{C,F} = 15.9 Hz), 125.57, 119.99, 118.02 (q, *J*_{C,F} = 296.7 Hz, TFA), 108.42, 56.36, 48.37, 45.57, 40.91, 22.90, 16.45. HRMS (ESI): Exact mass calculated for C₂₀H₂₆ClFN₇O₂S [M + H]⁺: 482.1536; found, 482.1534.

4.3. Radiochemistry. No carrier-added [^{11}C]CO₂ was produced by the ¹⁴N(*p*,α)¹¹C nuclear reaction using a GE

Healthcare PETtrace 800 cyclotron. The target gas (N₂ + 1% O₂) was used to transfer the contents of the irradiated target to the Procab, where [^{11}C]CO₂ was captured on a column containing molecular sieves (4 Å, 80/100 mesh). The column was flushed and heated to 350 °C to transfer the [^{11}C]CO₂ to the TRACERlab FX2 C radiosynthesizer. The [^{11}C]CO₂ was transferred to the sample loop, which contained the radiochemical precursor **2** and BEMP in DMF. A radioactivity detector proximal to the loop reactor was used to monitor the gas transfer. A solution of 1–10% (v/v) CH₃I in CH₃CN (300 μL) was added followed by CH₃CN (500 μL) and H₂O + 0.1% TFA (2 mL). The reaction mixture was loaded into the sample loop using helium gas and the TRACERlab FX2 C fluid detector and was injected onto the semi-preparative HPLC (flow rate: 7.5 mL min⁻¹; 32% CH₃CN/H₂O + 0.1% TFA). The fraction containing [^{11}C]encorafenib was collected into a vessel containing water (20 mL), and helium was used to transfer the solution through a preconditioned Sep-Pak C18 plus short cartridge. The cartridge was washed with water (15 mL), and [^{11}C]encorafenib was eluted into a vial with ethanol (1 mL), followed by 0.9% saline (9 mL). Helium gas was used to pass the solution through a filter (0.2 μm) into a final product vial. An aliquot of the final product was analyzed by analytical radio HPLC (flow rate: 1.0 mL min⁻¹; 5% CH₃CN/H₂O + 0.01% HCO₂H from 0 to 1 min, 5 to 95% CH₃CN/H₂O + 0.01% HCO₂H from 1 to 10 min, 95% CH₃CN/H₂O + 0.01% HCO₂H from 10 to 12 min) to determine the radiochemical and chemical purity. The chemical identity was confirmed using analytical HPLC by a coinjection of [^{11}C]encorafenib with **1**. The molar activity was measured by comparing the analytical HPLC UV (220 nm) response of the final product with a standard curve of **1**. The trapping efficiency of [^{11}C]CO₂ in the loop was determined by measuring the activity captured by the ascarite trap connected to the waste ports.

4.4. Cell Uptake Assay. A375 cells were plated at a density of 50,000 cells/well on 6-well cell culture plates and were grown to 80–90% confluence. The cells were washed with DPBS, and fresh media were added to each well. For the control group, a solution (1 mL) of [^{11}C]encorafenib (2 nM) in media was added (*n* = 3). For the blocked group, a solution (1 mL) of [^{11}C]encorafenib (2 nM) and nonradioactive encorafenib (5 μM) in media was added (*n* = 3). After incubation for 45 min at 37 °C, the media were removed, and the cells were washed with DPBS (3 × 2 mL), lysed with 0.1 M NaOH + 1% sodium dodecyl sulfate (0.6 mL), transferred to tubes, and measured with a γ-counter along with standards of [^{11}C]encorafenib prepared by serial dilution. The amount of protein in each sample was quantified using the micro BCA protein assay kit. The percent of the injected dose per milligram of protein (%ID/mg) was calculated from the decay-corrected counts and results from the BCA assay. Results are presented as mean ± standard deviation, and a two-tailed *t*-test was used to compare the control and blocked groups. *P* < 0.05 was considered significant.

■ AUTHOR INFORMATION

Corresponding Author

Mark H. Dornan – Department of Imaging, Dana-Farber Cancer Institute & Department of Radiology, Harvard Medical School, Boston, Massachusetts 02115, United States; Laboratoire de Radiochimie et Cyclotron, Centre de Recherche du Centre Hospitalier de l'Université de Montréal &

Département de Radiologie, radiooncologie et médecine nucléaire, Faculté de médecine, Université de Montréal, Montréal, Québec H3T 1J4, Canada; orcid.org/0000-0001-7611-3974; Email: MarkH_Dornan@dfci.harvard.edu

Authors

Daniil Petrenyov – Laboratoire de Radiochimie et Cyclotron, Centre de Recherche du Centre Hospitalier de l'Université de Montréal & Département de Radiologie, radiooncologie et médecine nucléaire, Faculté de médecine, Université de Montréal, Montréal, Québec H3T 1J4, Canada; orcid.org/0000-0002-6744-8630

José-Mathieu Simard – Laboratoire de Radiochimie et Cyclotron, Centre de Recherche du Centre Hospitalier de l'Université de Montréal & Département de Radiologie, radiooncologie et médecine nucléaire, Faculté de médecine, Université de Montréal, Montréal, Québec H3T 1J4, Canada

Mehdi Boudjemline – Laboratoire de Radiochimie et Cyclotron, Centre de Recherche du Centre Hospitalier de l'Université de Montréal & Département de Radiologie, radiooncologie et médecine nucléaire, Faculté de médecine, Université de Montréal, Montréal, Québec H3T 1J4, Canada

Roxana Mititelu – Division of Dermatology, Department of Medicine, McGill University, Montreal, Quebec H4A 3J1, Canada

Jean N. DaSilva – Laboratoire de Radiochimie et Cyclotron, Centre de Recherche du Centre Hospitalier de l'Université de Montréal & Département de Radiologie, radiooncologie et médecine nucléaire, Faculté de médecine, Université de Montréal, Montréal, Québec H3T 1J4, Canada; orcid.org/0000-0003-3637-3223

Anthony P. Belanger – Department of Imaging, Dana-Farber Cancer Institute & Department of Radiology, Harvard Medical School, Boston, Massachusetts 02115, United States

Complete contact information is available at: <https://pubs.acs.org/10.1021/acsoomega.0c02419>

Notes

The authors declare no competing financial interest.

ACKNOWLEDGMENTS

The authors thank the staff from the Molecular Cancer Imaging Facility at the Dana-Farber Cancer Institute and the Radiochemistry and Cyclotron Platform at the CRCHUM for radioisotope production. Fleur Gaudette of the CRCHUM Pharmacokinetics core facility performed high resolution and accurate mass measurements. This work was supported with a grant from the Friends of Dana-Farber Cancer Institute.

REFERENCES

- (1) Karimkhani, C.; Green, A. C.; Nijsten, T.; Weinstock, M. A.; Dellavalle, R. P.; Naghavi, M.; Fitzmaurice, C. The Global Burden of Melanoma: Results from the Global Burden of Disease Study 2015. *Br. J. Dermatol.* **2017**, *177*, 134–140.
- (2) Dimitriou, F.; Krattinger, R.; Ramelyte, E.; Barysch, M. J.; Micalletto, S.; Dummer, R.; Goldinger, S. M. The World of Melanoma: Epidemiologic, Genetic, and Anatomic Differences of Melanoma Across the Globe. *Curr. Oncol. Rep.* **2018**, *20*, 87.
- (3) Siegel, R. L.; Miller, K. D.; Jemal, A. Cancer Statistics. *CA. Cancer J. Clin.* **2019**, *69*, 7–34.
- (4) Zaman, A.; Wu, W.; Bivona, T. G. Targeting Oncogenic Braf: Past, Present, and Future. *Cancers* **2019**, *11*, 1197.
- (5) Ardekani, G. S.; Jafarnejad, S. M.; Khosravi, S.; Martinka, M.; Ho, V.; Li, G. Disease Progression and Patient Survival Are

Significantly Influenced by BRAF Protein Expression in Primary Melanoma. *Br. J. Dermatol.* **2013**, *169*, 320–328.

(6) Hugdahl, E.; Kalvenes, M. B.; Puntervoll, H. E.; Ladstein, R. G.; Akslen, L. A. BRAF-V600E Expression in Primary Nodular Melanoma Is Associated with Aggressive Tumour Features and Reduced Survival. *Br. J. Cancer* **2016**, *114*, 801–808.

(7) Bhandaru, M.; Ardekani, G. S.; Zhang, G.; Martinka, M.; McElwee, K. J.; Li, G.; Rotte, A. A Combination of p300 and Braf Expression in the Diagnosis and Prognosis of Melanoma. *BMC Cancer* **2014**, *14*, 398.

(8) Betancourt, L. H.; Szasz, A. M.; Kuras, M.; Murillo, J. R.; Sugihara, Y.; Pla, I.; Horvath, Z.; Pawlowski, K.; Rezeli, M.; Miharada, K.; Gil, J.; Eriksson, J.; Appelqvist, R.; Miliotis, T.; Baldetorp, B.; Ingvar, C.; Olsson, H.; Lundgren, L.; Horvatovich, P.; Welinder, C.; Wieslander, E.; Kwon, H. J.; Malm, J.; Nemeth, I. B.; Jönsson, G.; Fenyö, D.; Sanchez, A.; Marko-Varga, G. The Hidden Story of Heterogeneous B-Raf V600E Mutation Quantitative Protein Expression in Metastatic Melanoma—association with Clinical Outcome and Tumor Phenotypes. *Cancers* **2019**, *11*, 1981.

(9) Greaves, W. O.; Verma, S.; Patel, K. P.; Davies, M. A.; Barkoh, B. A.; Galbincea, J. M.; Yao, H.; Lazar, A. J.; Aldape, K. D.; Medeiros, L. J.; Luthra, R. Frequency and Spectrum of BRAF Mutations in a Retrospective, Single-Institution Study of 1112 Cases of Melanoma. *J. Mol. Diagn.* **2013**, *15*, 220–226.

(10) Cheng, L.; Lopez-Beltran, A.; Massari, F.; MacLennan, G. T.; Montironi, R. Molecular Testing for BRAF Mutations to Inform Melanoma Treatment Decisions: A Move toward Precision Medicine. *Mod. Pathol.* **2018**, *31*, 24–38.

(11) Delord, J.-P.; Robert, C.; Nyakas, M.; McArthur, G. A.; Kudchakar, R.; Mahipal, A.; Yamada, Y.; Sullivan, R.; Arance, A.; Kefford, R. F.; Carlino, M. S.; Hidalgo, M.; Gomez-Roca, C.; Michel, D.; Seroutou, A.; Aslanis, V.; Caponigro, G.; Stuart, D. D.; Moutouh-de Parseval, L.; Demuth, T.; Dummer, R. Phase I Dose-Escalation and -Expansion Study of the BRAF Inhibitor Encorafenib (LGX818) in Metastatic BRAF-Mutant Melanoma. *Clin. Cancer Res.* **2017**, *23*, 5339–5348.

(12) Koelblinger, P.; Thuerigen, O.; Dummer, R. Development of Encorafenib for BRAF-Mutated Advanced Melanoma. *Curr. Opin. Oncol.* **2018**, *30*, 125–133.

(13) Braftovi Product Label. U.S. Food and Drug Administration Website. https://www.accessdata.fda.gov/drugsatfda_docs/label/2018/2104961bl.pdf June 27, 2018. (Accessed April 7, 2020).

(14) Shimoda, Y.; Yui, J.; Fujinaga, M.; Xie, L.; Kumata, K.; Ogawa, M.; Yamasaki, T.; Hatori, A.; Kawamura, K.; Zhang, M.-R. [11C-carbonyl]CEP-32496: Radiosynthesis, Biodistribution and PET Study of Brain Uptake in P-gp/BCRP Knockout Mice. *Bioorg. Med. Chem. Lett.* **2014**, *24*, 3574–3577.

(15) Jiang, C.; Xie, L.; Zhang, Y.; Fujinaga, M.; Mori, W.; Kurihara, Y.; Yamasaki, T.; Wang, F.; Zhang, M. R. Pharmacokinetic Evaluation of [11C]CEP-32496 in Nude Mice Bearing BRAF V600E Mutation-Induced Melanomas. *Mol. Imaging* **2018**, *17*, 153601211879595.

(16) Wang, M.; Gao, M.; Miller, K. D.; Zheng, Q.-H. Synthesis of 2,6-Difluoro-N-(3-[11C]methoxy-1H-pyrazolo[3,4-B] Pyridine-5-Yl)-3-(Propylsulfonamidio)benzamide as a New Potential PET Agent for Imaging of B-RafV600E in Cancers. *Bioorg. Med. Chem. Lett.* **2013**, *23*, 1017–1021.

(17) Slobbe, P.; Windhorst, A. D.; Adamzek, K.; Bolijn, M.; Schuit, R. C.; Heideman, D. A. M.; van Dongen, G. A. M. S.; Poot, A. J. Development of [11C]vemurafenib Employing a Carbon-11 Carbonylative Stille Coupling and Preliminary Evaluation in Mice Bearing Melanoma Tumor Xenografts. *Oncotarget* **2017**, *8*, 38337–38350.

(18) Wilson, A. A.; Garcia, A.; Houle, S.; Vasdev, N. Direct Fixation of [11C]-CO₂ by Amines: Formation of [11C-Carbonyl]-Methyl-carbamates. *Org. Biomol. Chem.* **2010**, *8*, 428–432.

(19) Downey, J.; Bongarzone, S.; Hader, S.; Gee, A. D. In-Loop Flow [11C]CO₂ Fixation and Radiosynthesis of N,N'-[11C]-dibenzylurea. *J. Labelled Compd. Radiopharm.* **2018**, *61*, 263–271.

(20) Dahl, K.; Collier, T. L.; Cheng, R.; Zhang, X.; Sadovski, O.; Liang, S. H.; Vasdev, N. "In-loop" [11C]CO₂ Fixation: Prototype and

Proof of Concept. *J. Labelled Compd. Radiopharm.* **2018**, *61*, 252–262.

(21) Capper, D.; Preusser, M.; Habel, A.; Sahm, F.; Ackermann, U.; Schindler, G.; Pusch, S.; Mechtersheimer, G.; Zentgraf, H.; von Deimling, A. Assessment of BRAF V600E Mutation Status by Immunohistochemistry with a Mutation-Specific Monoclonal Antibody. *Acta Neuropathol.* **2011**, *122*, 11–19.